Philosophical Magazine

ISSN: 1478-6435 (Print) 1478-6443 (Online) Journal homepage: https://www.tandfonline.com/loi/tphm20

The investigation of electronic, mechanical and lattice dynamical properties of PdCoX (X = Si and Ge) half-Heusler metallics in α, β and γ structural phases: an *ab initio* study

Aytaç Erkisi, Gokhan Surucu & Recai Ellialtioglu

To cite this article: Aytaç Erkisi, Gokhan Surucu & Recai Ellialtioglu (2017) The investigation of electronic, mechanical and lattice dynamical properties of PdCoX (X = Si and Ge) half-Heusler metallics in α, β and γ structural phases: an *ab initio* study, Philosophical Magazine, 97:26, 2237-2254, DOI: 10.1080/14786435.2017.1329595

To link to this article: https://doi.org/10.1080/14786435.2017.1329595

Published online: 22 May 2017.

Submit your article to this journal

Article views: 271

View related articles

View Crossmark data

Citing articles: 7 View citing articles

Full Terms & Conditions of access and use can be found at
https://www.tandfonline.com/action/journalInformation?journalCode=tphm20

PHILOSOPHICAL MAGAZINE, 2017
VOL. 97, NO. 26, 2237–2254
https://doi.org/10.1080/14786435.2017.1329595

Taylor & Francis
Taylor & Francis Group

Check for updates

The investigation of electronic, mechanical and lattice dynamical properties of PdCoX (X = Si and Ge) half-Heusler metallics in α, β and γ structural phases: an *ab initio* study

Aytaç Erkisi[a], Gokhan Surucu[b,c,d] and Recai Ellialtioglu[a]

[a]Department of Physics Engineering, Hacettepe University, Ankara, Turkey; [b]Department of Electric and Energy, Ahi Evran University, Kirsehir, Turkey; [c]Department of Physics, Middle East Technical University, Ankara, Turkey; [d]Photonics Application and Research Center, Gazi University, Ankara, Turkey

ABSTRACT

PdCoX (X = Si and Ge) alloys which are XYZ type half-Heusler alloys and also have face centred cubic MgAgAs-type structure which conforms to $F\bar{4}3m$ space group, have been investigated in different atomic arrangements which are called α, β and γ phases, using local spin density approximation in the density functional theory as implemented in VASP (Vienna *Ab Initio* Simulation Package) software. Both of the alloys are considered in ferromagnetic order. After the investigation of stable structural phase for these alloys, their full structural, electronic, magnetic, mechanical, and dynamical properties have been examined in this structural phase. The calculated electronic band structure and the total electronic density of states of our alloys indicated metallic behaviour. The estimated elastic constants show that these are stable and show anisotropic behaviour mechanically in β and γ phases. Also, the calculated phonon dispersion curves show that PdCoX (X = Si and Ge) alloys are stable dynamically in the same structural phases.

ARTICLE HISTORY
Received 9 August 2016
Accepted 7 May 2017

KEYWORDS
Half-Heusler; *ab initio* calculations; elastic constant; electronic band structure; phonon

1. Introduction

Half-Heusler (HH) alloys are unique in that they are natural prime candidates for use in topological insulator [1,2], spintronic [3,4], optoelectronic, photovoltaic applications [5], and thermoelectric materials [6,7] due to their wide variety of interesting physical properties [8]. The reason for their use in a wide range of applications is that these alloys have good electrical, mechanical and electronic properties and thermal stability [9].

CONTACT Aytaç Erkisi erkisi@hacettepe.edu.tr

© 2017 Informa UK Limited, trading as Taylor & Francis Group

Spin-polarised charge carriers are considered as the key ingredient for spintronics. The half-metallic materials such as half-metallic ferromagnets (HMFs) and half-metallic antiferromagnets are the most suitable choice for these carriers. The half-metallic materials have characteristic properties in their energy bands having semiconductor-like in one spin direction at the Fermi level, whereas in the other spin direction they are strongly metallic, i.e. 100% spin polarised conduction electrons at the Fermi level [4].

The HMFs were first discovered by theoretical band structure calculations for HH alloy NiMnSb [10]. Then, HH alloys have been examined in terms of three distinct atomic arrangements in the literature [7,11–18]. These alloys have $C1_b$ crystal structure conforms to $F\bar{4}3m$ space group and also are similar to the crystal structure of a full-Heusler alloy (X_2YZ) having $L2_1$ crystal structure, but with one missing X atom. The atomic arrangements in these compositions are called α, β and γ phases [13] and are given in Table 1. As seen in this table, X, Y and Z atoms occupy atomic positions in the different type structural phases are presented with the notation determined by Wyckoff [19].

The structure of the γ phase of HH alloys has been determined using X-ray diffraction [15] as the non-magnetic element Z atom being nearest neighbour to the Y atom in this arrangement. There are other works which studied the α phase of HH alloys [14,16], in which the X atom is nearest neighbour to both Z and Y atoms. In the β phase, Z atom is nearest neighbour to both X and Y atoms, which is determined by Larsen et al. [13]. It is well known that the α, β and γ phases in the HH alloys significantly influence the electronic and magnetic properties of such structures [20,21].

We chose PdCoSi and PdCoGe HH material systems, which have not been investigated before, to the best of our knowledge. The motivation for this is as follows. In addition to its hydrogen absorbing property, Pd and its binary alloys including PdCo have attracted great attention as being strong catalysts in anion exchange polymer electrolyte membrane fuel cells [22]. When diluted with Co, Pd shows giant ferromagnetism [23]. When used as Co_2MnSi/PdCo multilayer spacer in magnetic tunnel junctions, high values of spin polarisation is obtained with the aid of the perpendicular magnetic anisotropy of PdCo [24].

In this study, we have presented the results of our investigation on the structural, electronic, magnetic, mechanical and dynamic behaviours of PdCoX (X = Si and Ge) HH alloys which have face centered cubic structure ($F\bar{4}3m$), in different atomic arrangements so-called α, β and γ phases. The computational details are given in the second section. In the third section, the discussion of the examined

Table 1. The Wyckoff positions of the three atoms for α, β and γ phases. The corresponding positions are 4a: (0,0,0)*a*, 4b: (1/2,1/2,1/2)*a*, and 4c: (1/4,1/4,1/4)*a*, where *a* is the lattice constant.

Phase	X	Y	Z
α	4c	4b	4a
β	4b	4a	4c
γ	4a	4c	4b

and calculated structural and mechanical properties and also electronic band structure, lattice dynamical behaviours of our alloys in different α, β and γ phases are given. Finally, in the last section, we summarised our results with conclusion. To the extend we know, these detailed calculations have not been done before for the PdCoX alloys.

2. Computational details

For all the calculations in this work, linear augmented-plane-wave basis set and pseudopotential approximation is utilised in the VASP (**V**ienna ***Ab initio*** **S**imulation **P**ackage) [25,26] software. For approximating exchange-correlation potential, Projected Augmented Wave (PAW) [27,28] type pseudopotentials for all atoms in the framework of local spin density approximation (LSDA) of density functional theory (DFT) [29,30] functionals are used. The valence electron configurations of *Pd, Co, Si* and *Ge* atoms are considered as $4d^9 5s^1$, $3d^8 4s^1$, $3s^2 3p^2$ and $4s^2 4p^2$, respectively.

Our alloys have $C1_b$ crystal structure which conforms to $F\bar{4}3m$ space group. After the optimisation of our alloys in different α, β and γ phases, energy–volume graphics are plotted by fitting to Vinet equation of state. Then, their full structural, mechanical, electronic and lattice dynamical behaviours have been examined in each phase separately. The Brillouin zone integrations have been performed with automatically generated $8 \times 8 \times 8$ **k**-point mesh used in the irreducible Brillouin zone, all centered at Γ-point, following the convention of Monkhorst and Pack [31]. The chosen kinetic energy cut-off value is 1100 eV for wave functions in plane wave basis sets expansion of the eigenfunctions. The ionic relaxation process has been carried out until the successive change in the total energy is less than 10^{-9} eV. The forces and the pressure have been minimised in order to obtain the optimal lattice parameters and atomic positions in the primitive cell of the crystal in all three phases.

3. Results and discussion

Firstly, we investigated the stable structural phase for PdCoX (X = Si and Ge) alloys and the plotted three dimensional (3D) crystallographic representation of these alloys in α, β and γ phases are presented in Figure 1. For each phase, the primitive cell of structures is modelled by three atoms in the ferromagnetic order.

After the investigation of optimal structural parameters of these alloys in each phase, energy–volume graphics of these systems are plotted by fitting to Vinet [32] equation of state. Then, the mechanical properties, electronic band structure, and lattice dynamical properties of our alloys have been studied in α, β and γ phases which conforms to $F\bar{4}3m$ space group.

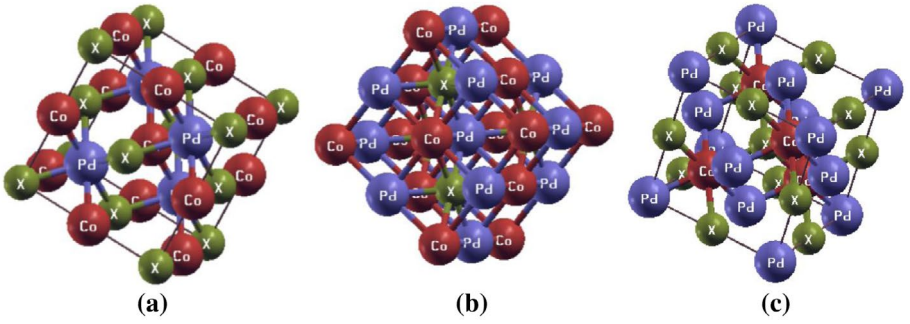

Figure 1. (colour online) The three dimensional (3D) crystallographic shape of half-Heusler PdCoX (X = Si and Ge) alloys in: (a) α phase, (b) β phase and (c) γ phase.

Table 2. The calculated cohesive and formation energies of half-Heusler PdCoX (X = Si and Ge) alloys in α, β and γ phase.

Compound	Phase	E_{coh} (eV/f.u.)	E_{for} (eV/f.u.)
PdCoSi	α	−16.887	−2.576
	β	−18.541	−4.230
	γ	−17.562	−3.251
PdCoGe	α	−15.917	−2.356
	β	−17.013	−3.452
	γ	−16.578	−3.017

3.1. Structural properties in α, β and γ phases

In this subsection, it has been presented the investigated energetically more favoured structural phase of PdCoX (X = Si and Ge) alloys. The calculated cohesive (E_{coh}) [33,34] and formation energies (E_{for}) [35] have provided which phase is energetically most stable for these alloys. If the calculated absolute values of cohesive and formation energies of a crystal in any structural phase are larger than that of other phases, that is the most stable and energetically more suitable phase. The cohesive and formation energies of a crystal with a chemical formula A_xB_y are given, respectively, by

$$E_{coh} = E_{tot} - \left(xE_A + yE_B\right) \tag{1}$$

and

$$E_{for} = E_{tot} - \left(xE_A^{bulk} + yE_B^{bulk}\right) \tag{2}$$

where, E_{tot} is the total energy of the unit cell of the crystal. E_A and E_B are the energy values of the isolated A and B atoms. $E_A^{bulk}$and E_B^{bulk} are the ground state energy values of A and B atoms in their bulk crystal form. The calculated cohesive and formation energies of our alloys in each phase are given in Table 2. The absolute value of cohesive and formation energies of the β phase are larger than that of

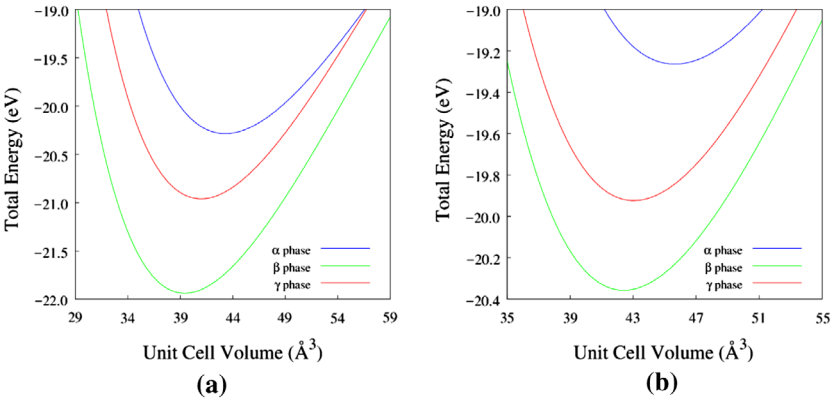

Figure 2. (colour online) Total energies of unit cell as a function of volume in three different type structural phase: (a) PdCoSi, (b) PdCoGe.

Table 3. The optimised structural parameters of half-Heusler PdCoX (X = Si and Ge) alloys within LSDA in α, β and γ phase.

Material	Phase	a (Å)	B (GPa)	B'
PdCoSi	α	5.572	173.99	4.91
	β	5.401	208.72	4.68
	γ	5.472	198.92	4.80
PdCoGe	α	5.672	158.31	5.05
	β	5.535	190.08	4.94
	γ	5.562	184.08	4.89

the others and so it is the most suitable phase for these alloys. Also, it is shown in Table 2 that all alloys are energetically stable due to the negative formation enthalpy values, indicating that they should be possible to synthesise the considered phases. Among these phases, PdCoSi (β phase) (−18.541 eV/f.u.) is found to be relatively the most stable one.

After obtaining ground state volume and energy values of PdCoX (X = Si and Ge) alloys in each phase within LSDA, energy–volume curves are plotted as seen in Figure 2 and the lattice parameters, bulk modulus and their pressure derivatives are calculated by fitting the Vinet equation of state [32] which is given in Equation (3). A well-converged ground state is obtained for each of our alloys, with the asymptotic standard errors in fitting process being less than about 1%. The calculated lattice parameters and some structural constants for each phase are given in Table 3.

$$E(V) = E_0 + \frac{9BV_0}{\xi^2}\left[1 + \{\xi(1-x) - 1\}\exp\{\xi(1-x)\}\right] \tag{3}$$

where E_0 and V_0 are the ground state energy and volume, respectively, $\xi = (3/2)\left(B' - 1\right)$, with B being the bulk modulus and B' is its pressure derivative, and $x = \left(V/V_0\right)^{1/3}$.

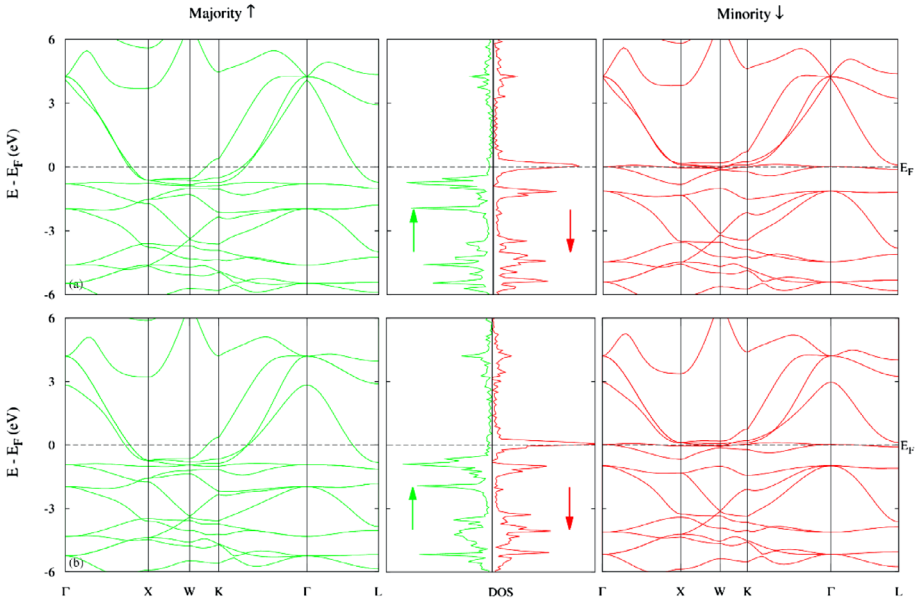

Figure 3. (colour online) For α phase, the calculated energy band structures and the total density of electronic states (DOS) within LSDA for (a) PdCoSi, (b) PdCoGe alloys. The zero of band energy is shifted to Fermi level (E_F).

The fitted energy–volume curves of PdCoX (X = Si and Ge) alloys show that, they are the most stable in β phase and energetically the secondary suitable phase is the γ phase, as can be seen in Figure 2. The lattice parameters are the smallest in β phase and the largest in α phase as given in Table 3. Bulk moduli are larger in β phase than the other structural phases. Also, they have large pressure derivatives of bulk moduli, especially in α phase. This indicates that these alloys show strong sensitivity against pressure change in all structural phases.

3.2. *Electronic and magnetic properties*

The electronic behaviour of a material can be determined with electronic band structure and density of states (DOS) of materials. The calculated electronic band structures and total density of states of PdCoX (X = Si and Ge) alloys in both majority (up) and minority (down) spin channels using LSDA are separately shown along the high symmetry lines in the first Brillouin zone for α, β and γ phases, respectively, in Figures 3–5. It is obvious that, both of our materials show metallic property since there is no band gap neither for up nor for down spin channels in electronic band structures for all phases. Moreover, our materials are close to ferromagnetic nature only in α phase and non-magnetic in β and γ phases due to the fact that up and down spin channels in electronic band structures are almost the same for our alloys in these phases. This situation is well in agreement with total magnetic moment of our alloys as seen in Table 4.

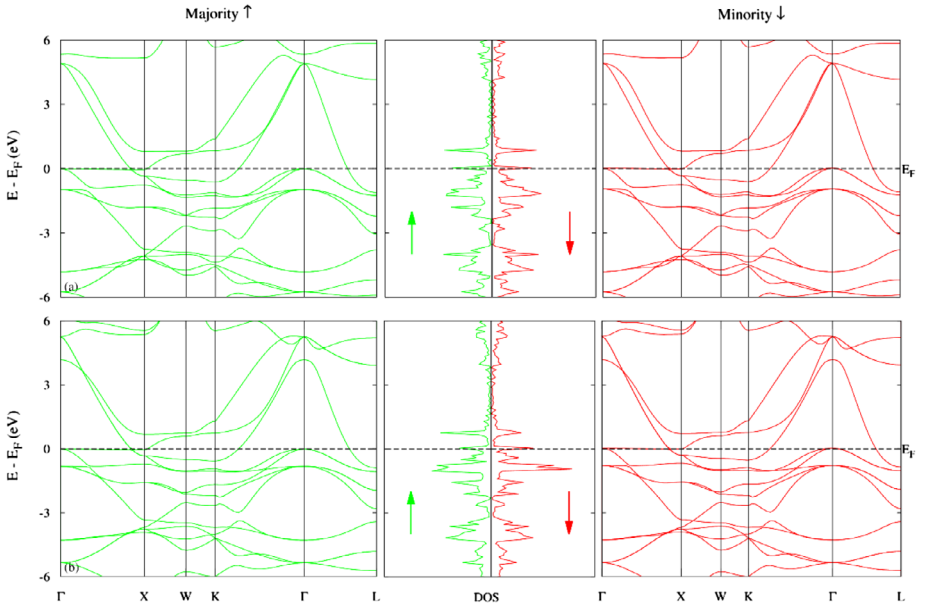

Figure 4. (colour online) For β phase, the calculated energy band structures and the total density of electronic states (DOS) within LSDA for (a) PdCoSi, (b) PdCoGe alloys. The zero of band energy is shifted to Fermi level (E_F).

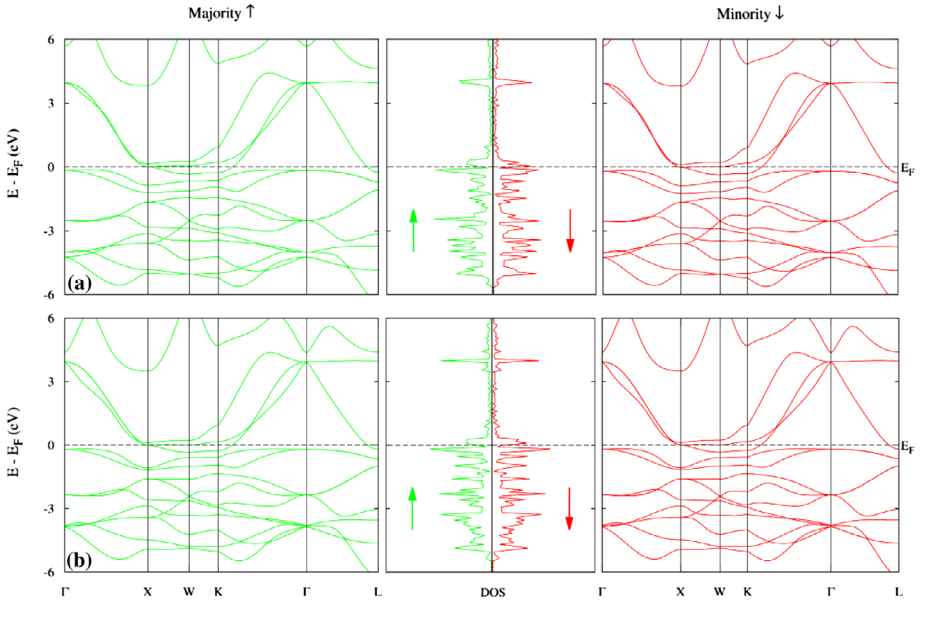

Figure 5. (colour online) For γ phase, the calculated energy band structures and the total density of electronic states (DOS) within LSDA for (a) PdCoSi, (b) PdCoGe alloys. The zero of band energy is shifted to Fermi level (E_F).

Table 4. The total magnetic moments of half-Heusler PdCoX (X = Si and Ge) alloys and partial magnetic moment of the atoms in composition within LSDA in α, β and γ phase.

Material	Phase	$\mu_{tot}(\mu_B)$	$\mu_{atom}(\mu_B)$
PdCoSi	α	1.174	$\mu_{Pd} = 0.080$ $\mu_{Co} = 1.111$ $\mu_{Si} = -0.018$
	β	0.037	$\mu_{Pd} = 0.003$ $\mu_{Co} = 0.034$ $\mu_{Si} = 0.000$
	γ	−0.068	$\mu_{Pd} = -0.015$ $\mu_{Co} = -0.055$ $\mu_{Si} = 0.002$
PdCoGe	α	1.373	$\mu_{Pd} = 0.101$ $\mu_{Co} = 1.299$ $\mu_{Ge} = -0.027$
	β	0.055	$\mu_{Pd} = 0.001$ $\mu_{Co} = 0.055$ $\mu_{Ge} = -0.001$
	γ	0.015	$\mu_{Pd} = 0.003$ $\mu_{Co} = 0.012$ $\mu_{Ge} = -0.000$

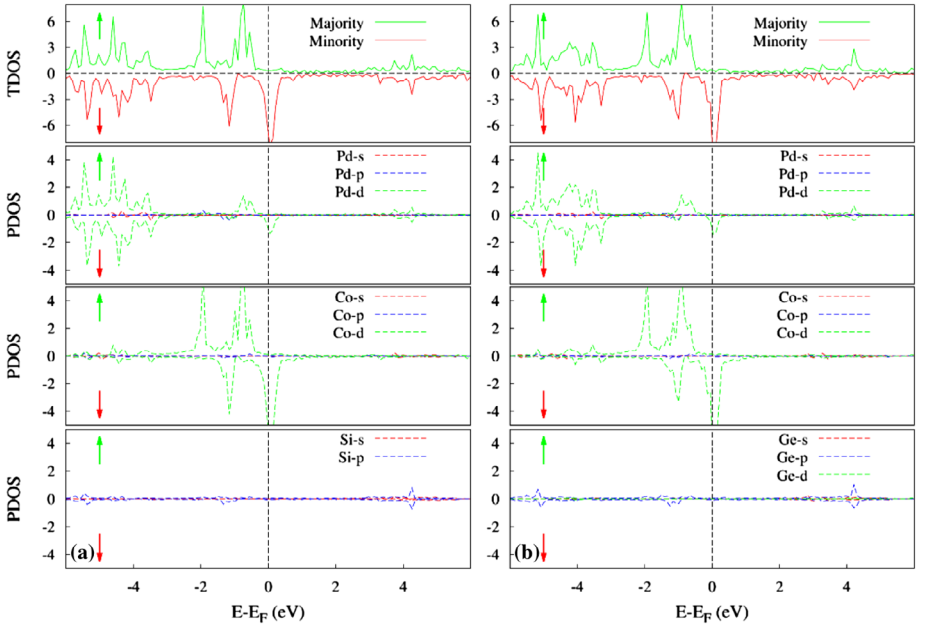

Figure 6. (colour online) The total and orbital projected partial density of electronic states of atoms within LSDA in α phase for (a) PdCoSi and (b) PdCoGe compound.

The calculated orbital projected partial density of electronic states of atoms in PdCoX (X = Si and Ge) alloys in α, β and γ phases are given in Figures 6–8, respectively. For all three phases, 3d states of Co atoms and 4d states of Pd atoms cross the Fermi level (E_F), yielding a metallic behaviour. In addition, we see that the d orbitals of Pd atoms are located between −4 and −6 eV below E_F, that's why it has no remarkable effect on bonding features of the systems. In this respect,

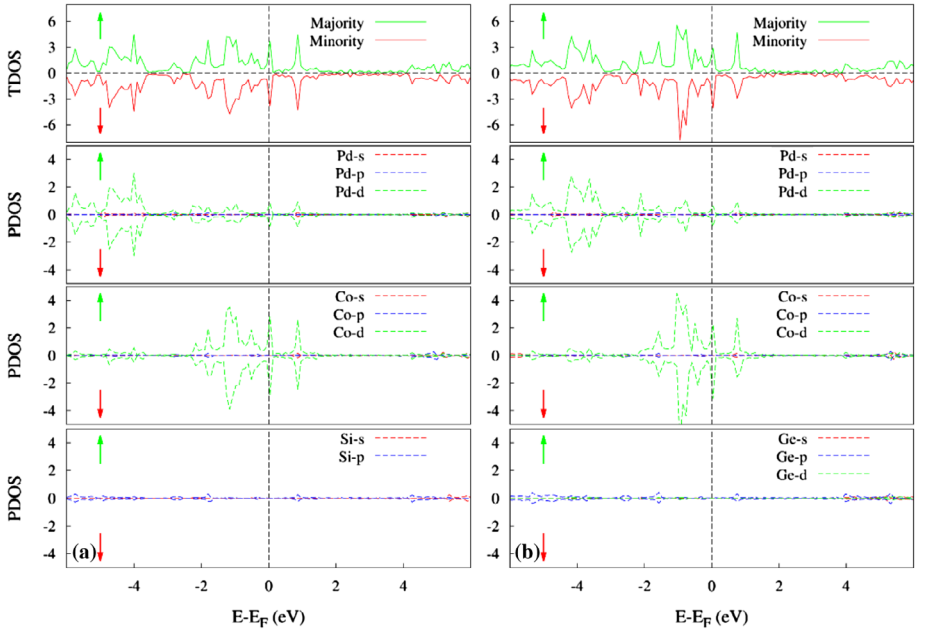

Figure 7. (colour online) The total and orbital projected partial density of electronic states of atoms within LSDA in β phase for (a) PdCoSi and (b) PdCoGe compound.

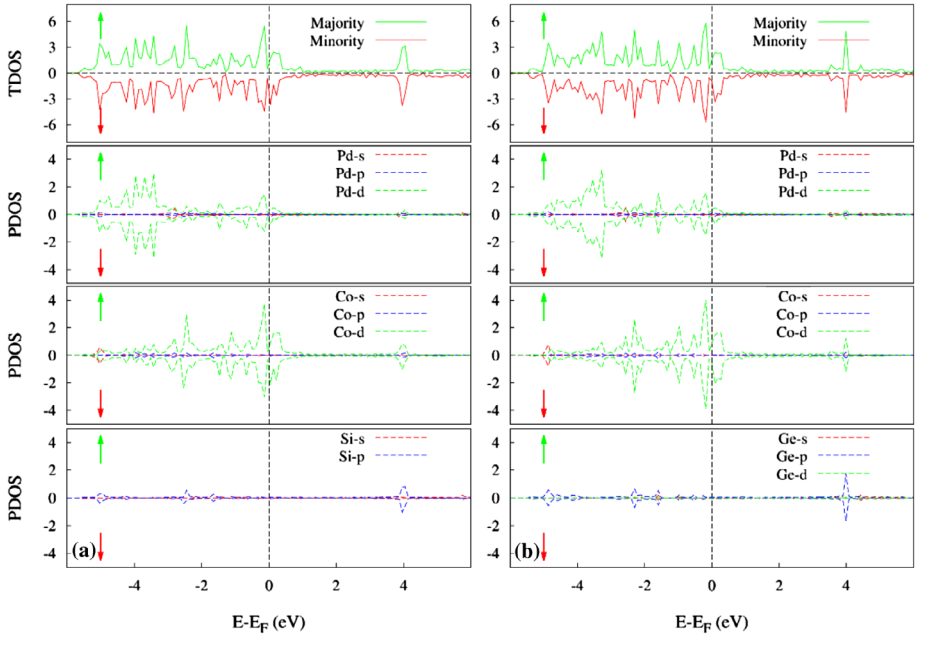

Figure 8. (colour online) The total and orbital projected partial density of electronic states of atoms within LSDA in γ phase for (a) PdCoSi and (b) PdCoGe compound.

Table 5. The calculated elastic constants of PdCoX (X = Si and Ge) alloys in α, β and γ phase.

Material	Phase	C_{11} (GPa)	C_{12} (GPa)	C_{44} (GPa)
PdCoSi	α	156.03	192.33	−54.14
	β	349.53	136.57	58.35
	γ	242.85	174.32	4.74
PdCoGe	α	122.79	167.18	−17.33
	β	279.12	144.70	44.71
	γ	233.11	158.71	16.71

Table 6. The calculated upper and lower limits, average values of bulk and shear moduli, Young's moduli and Poisson's ratios of PdCoX (X = Si and Ge) alloys in stable β and γ phase.

Material	Phase	B (GPa)	G_V (GPa)	G_R (GPa)	G (GPa)	B/G	v	E (GPa)
PdCoSi	β	207.56	77.60	71.23	74.42	2.79	0.340	199.42
	γ	197.17	16.55	7.23	11.89	16.59	0.470	34.96
PdCoGe	β	189.50	53.71	51.62	52.66	3.60	0.373	144.60
	γ	183.51	24.90	21.43	23.16	7.92	0.439	66.69

Table 7. The calculated shear anisotropy factors (A and $A\_$) and longitudinal (v_l), transverse (v_t), and average (v_m) wave velocities in crystal and also Debye temperatures (θ_D) of PdCoX (X = Si and Ge) in β and γ phases.

Material	Phase	A	$A\_$	v_l (m/s)	v_t (m/s)	v_m (m/s)	θ_D (K)
PdCoSi	β	0.548	0.622	6135.1	3021.6	3392.7	428.1
	γ	0.138	0.178	5213.1	1231.5	1406.7	175.2
PdCoGe	β	0.665	0.728	5279.9	2377.6	2681.4	330.2
	γ	0.449	0.523	4832.1	1588.3	1807.5	221.5

the metallicity of these systems can be attributed to 3d states of Co atom in our compositions for all structural phases. Therefore, the bonding properties of PdCoX (X = Si and Ge) alloys are due to the hybridisation between d-orbitals of Pd and Co atoms.

On the other hand, the total and partial magnetic moments for all phases are calculated, and they are listed in Table 4. It is clearly seen that the main contribution to the total magnetic moment for both alloys comes from Co atom. Since the total magnetic moment in PdCoX (X = Si and Ge)-α phases are greater than 1, it can be said that these materials show ferromagnetic properties. On the contrary, for non-magnetic materials it is zero or very close to zero. Our materials are close to ferromagnetic nature only in α phase, and non-magnetic in β and γ phases. The total magnetic moment values obtained for PdCoX agree well with the above shown electronic band structures.

3.3. Elastic constants and some mechanical properties in α, β and γ phases

Elastic constants (C_{ij}) of a crystal are very important and valuable due to their use in estimating the mechanical properties and dynamical stability of the crystal, such as stability, hardness or stiffness and also sound velocities and Debye temperatures. These values can be calculated with high accuracy and precision

in *ab initio* calculations using the 'stress–strain' method [36]. Three independent elastic constants of a cubic crystal are C_{11}, C_{12} and C_{44} and these constants for PdCoX (X = Si and Ge) alloys in each structural phase are presented in Table 5.

The mechanical stability of a crystal, in other words the durability of the crystal against external forces, is a desirable property in order to ensure its sustainability in any application. Mechanical stability is determined according to the Born–Huang criteria [37]. This criteria check for the strain energy against any homogeneous elastic deformation and the value of this energy must be positive [38]. There are three independent elastic constants for a cubic crystal and Born's mechanical stability criteria of a cubic crystal are shown in Equation (4).

$$C_{11} - C_{12} > 0; \quad C_{11} + 2C_{12} > 0; \quad C_{11} > 0 \text{ and } C_{44} > 0 \tag{4}$$

PdCoX (X = Si and Ge) alloys are stable mechanically in both β and γ phase according to the above-mentioned stability criteria. Both of our alloys are mechanically unstable in α phase, because of the negative elastic constants. Hence, further mechanical properties depending on elastic constants of PdCoX (X = Si and Ge) alloys have been examined only for β and γ structural phases. Among the elastic constants of a cubic crystal, C_{44} gives information about the shear resistance in [1 0 0] direction. The atomic bonding in this direction for β phase is between Pd and Co atoms and it is between Pd and X (X = Si and Ge) atoms for γ phase. Since C_{44} values are largest, the β phase is the most stable phase and Pd-Co bond is the strongest bond in this phase, especially for PdCoSi alloy. In the γ phase, the value of C_{44} indicates that Pd–Ge bonding is larger than Pd–Si bonding, as seen in Table 5. C_{11}–C_{12} value is related to the stiffness with a shear in [1 1 0] direction too. For β phase, the bonding in this direction is weaker for PdCoGe than that for PdCoSi. For secondary stable γ phase, the bonding strength in this direction is similar for both of our alloys.

The Cauchy pressure (P_C) as given in Equation (5), can determine the angular character of atomic bonding in alloys [38,39]

$$P_C = C_{12} - C_{44} \tag{5}$$

If the Cauchy pressure of a cubic crystal is negative ($C_{12} < C_{44}$), that ensures the atomic bonding nature of this crystal is covalent type. On the other hand, if this pressure is positive ($C_{44} < C_{12}$) the atomic bonding nature is metallic-like. Also the Cauchy relation ($C_{12} = C_{44}$) is approximately provided for ionic crystals and some metals [40] when there is no external pressure. The calculated P_C values of PdCoX (X = Si and Ge) alloys in β and γ structural phases are positive and this situation indicates that, the bonding nature of PdCoX alloys in both of two structural phases is metallic.

Additionally, some mechanical properties of a crystal can be estimated from the calculated elastic constants. The bulk (B) and shear moduli (G) of a crystal can be estimated from Voigt–Reuss–Hill relations [41–43]. For a cubic crystal, the upper and lower limits of B are equal to the each other as seen in Equation (6)

and also G_V (upper limit of G) and G_R (lower limit of G) values can be estimated using the Voigt and Reuss approximations as in Equations (7) and (8), respectively.

$$B_V = B_R = B = (C_{11} + 2C_{12})/3 \tag{6}$$

$$G_V = \left(C_{11} - C_{12} + 3C_{44}\right)/5 \tag{7}$$

$$G_R = 5\left(C_{11} - C_{12}\right)C_{44}/\left(4C_{44} + 3C_{11} - 3C_{12}\right) \tag{8}$$

The average values of bulk and shear moduli of a crystal can be calculated from Hill approximations which are given by $B = (1/2)\left(B_V + B_R\right)$and $G = (1/2)\left(G_V + G_R\right)$, respectively.

Moreover, Poisson's ratio (ν) and Young's modulus (E) of a crystal [38] have been calculated using bulk and shear moduli as seen in Equations (9) and (10), respectively.

$$\nu = (3B - 2G)/[2(3B + G)] \tag{9}$$

$$E = (9BG)/(3B + G) \tag{10}$$

For PdCoX (X = Si and Ge) alloys in β and γ phase, the calculated bulk moduli, the upper and lower limits of shear moduli using Voigt and Reuss approximations, respectively, the calculated average shear moduli using Hill approximation and the calculated Young's modulus using Equation (10), B/G ratio and the calculated Poisson's ratios using Equation (9) have been presented in Table 5. The values of B/G ratio of PdCoX (X = Si and Ge) alloys show that, these alloys are largely ductile materials in both of β and especially γ phases, as seen in Table 6. Because, the values of B/G is higher than 1.75 refer ductility, while lower values indicate brittleness [44].

Poisson's ratios of PdCoX (X = Si and Ge) alloys in β phase are found to be 0.340 and 0.373, respectively, and 0.470 and 0.439, respectively, in γ phase as seen in Table 6. These values show that the bonding character of our materials is close to metallic when they are in β and γ phase [45]. For platinum-based bulk metallic glasses, for example, which represent some of the densest metals because of the variety of atom sizes, $\nu \to 0.5$ [46]. Also, these ratios indicate that our materials can be compressed more easily in γ phase than in β phase.

Young's modulus which is used to determine the stiffness of a solid is given as the ratio of stress and strain [47]. The calculated values of shear, and Young's moduli of our alloys in β and γ phases show that both of our materials are harder in β phase than the secondary stable γ phase.

The anisotropic or isotropic behaviour of a material can be determined from shear anisotropy factors [48] associated with it. They can be calculated using Equations (11) and (12) for a cubic crystal and are given in Table 6. For the {1 1 0}

planes of a cubic crystal, the value of $A\_$ is not independent from A. However, it does reduce to A when it satisfies the elastic isotropy condition $\left(2C_{44} = C_{11} - C_{12}\right)$ [48]. The respective shear anisotropy factors (A and $A\_$) in {1 0 0} and {1 1 0} planes for a cubic crystal are given by

$$\mathrm{A} = 2C_{44}/\left(C_{11} - C_{12}\right) \tag{11}$$

$$A\_ = C_{44}\left(C_L + 2C_{12} + C_{11}\right)/\left(C_L C_{11} - C_{12}^2\right) \tag{12}$$

where $C_L = C_{44} + \left(C_{11} + C_{12}\right)/2$.

We can deduce from Table 7 that the shear anisotropy values A_ and A of both alloys in both phases are greater for (1 1 0) plane than that for (1 0 0) plane. These calculated values indicate that, our alloys have rather strong anisotropic character when they are in γ phase, but in the most stable structural phase (β phase), PdCoGe compound has weaker anisotropic character than PdCoSi compound mechanically.

Navier's equation [49] can be used for calculating longitudinal and transverse wave velocities and also average wave velocity [50] of a crystal, given by Equations (13)–(15), respectively.

$$v_{\mathrm{l}} = \left[(B + (4G/3))/\rho\right]^{1/2} \tag{13}$$

$$v_{\mathrm{t}} = \left[G/\rho\right]^{1/2} \tag{14}$$

$$v_{\mathrm{m}} = \left\{(1/3)\left[\left(2/\left(v_{\mathrm{t}}^3\right)\right) + \left(1/\left(v_{\mathrm{l}}^3\right)\right)\right]\right\}^{-1/3} \tag{15}$$

where ρ is the density of the material. Moreover, sound conductivity for both alloys is greater in the stable β phase than in γ phase. Sound velocity values of PdCoSi are greater than that of PdCoGe in both phases, as seen in Table 7.

Equation (16) gives the Debye temperature of a compound (θ_{D}) which is an important fundamental parameter in relation with many physical properties such as specific heat and melting temperature [51].

$$\theta_{\mathrm{D}} = (h/k)\left[(3n/4\pi)\left(N_{\mathrm{A}}\rho/M\right)\right]^{1/3} v_{\mathrm{m}} \tag{16}$$

where h is the Planck's constant, k the Boltzmann's constant, N_{A} is the Avogadro's number, M is the molecular weight and n is the number of atoms in the molecule. The calculated Debye temperatures of PdCoX (X = Si and Ge) alloys are presented in Table 7. One sees that the β phase values are higher than γ phase values. We note that the β phase value of PdCoSi is (428.1 K) higher than that

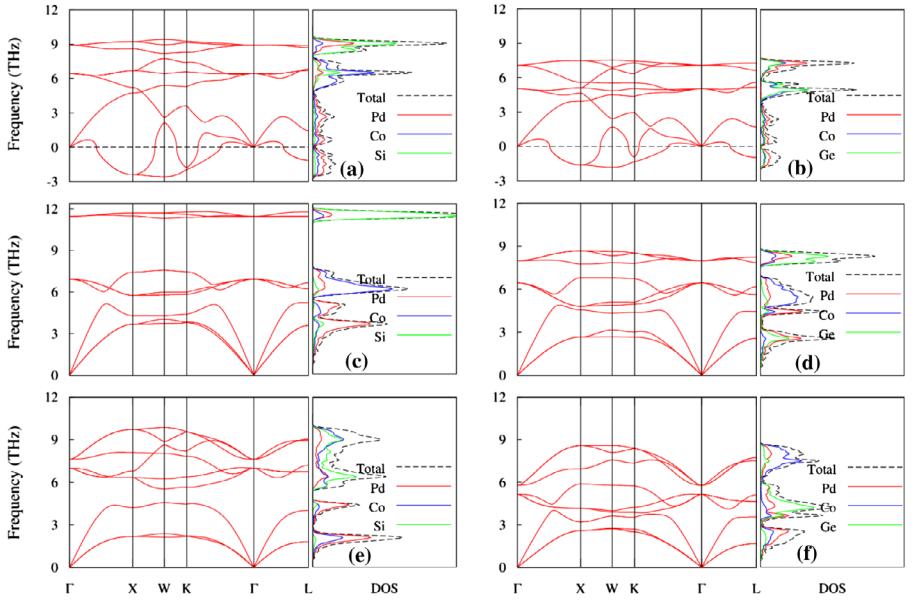

Figure 9. (colour online) Phonon dispersion curves along high symmetry directions in the first Brillion zone and vibrational density of states (DOS) of (a) PdCoSi in α phase, (b)PdCoGe in α phase, (c) PdCoSi in β phase and (d) PdCoGe in β phase, (e) PdCoSi in γ phase and (f) PdCoGe in γ phase.

(330.2 K) of PdCoGe, whereas it is the other way around in the γ phase; (175.2 K) and (221.5 K), respectively.

3.4. The lattice dynamical properties

Finally, in this subsection, we have presented the calculated lattice dynamical properties of PdCoX (X = Si and Ge) alloys. We have examined the phonon dispersion spectra of our alloys in each structural phase to decide on the structural stability of these materials. We used the program PHONOPY [52] to calculate the phonon frequencies of our alloys based on the interatomic force constants. We obtained the force constants and vibrational frequencies using the linear response method within the density functional perturbation theory [52–55]. For calculating full phonon spectra along the high symmetry directions in the irreducible Brillouin zone, which are presented along with the atom projected vibrational density of states, 2 × 2 × 2 super-cells were formed for PdCoX (X = Si and Ge) alloys in all phases, as seen in Figure 9(a)–(f). To the best of our knowledge, there is no study in the literature examining the vibrational properties of these alloys, so there is no data to compare.

It has been clearly seen that the calculated phonon dispersion spectra of both of our alloys do not show any softening behaviour in most stable β and secondary stable γ structural phases as expected, except at Γ point, as seen in Figure 9(a)–(e). Hence, PdCoX (X = Si and Ge) alloys are dynamically stable in β and γ phases but

unstable in α phase. This situation is in agreement with Section 3.2. Each compound, being composed of three atoms, has a total of nine phonon branches, three acoustic and six optical. There is a clear gap in the calculated phonon dispersion curves between the optic and acoustic branches for PdCoSi, both in β and γ phases due to the low atomic mass of Si, as seen in Figure 9(c)–(e). The observed gaps of PdCoSi compound in β and γ phases are around 0.59 and 0.95 THz, respectively. There are sharper peaks of the optical vibrations of Pd atom at low energy regions, somewhere between 1.3 THz and 7.7 THz, because of its higher atomic mass and the optical mode energies are comparable to its acoustic branch energies. Also, the optical modes of Si atom are located at a wide energy range between 5.4 and 9.9 THz due to the lower atomic mass of Si atom and also especially for β phase, there is a sharp peak around 12 THz in optical modes of Si atom.

4. Conclusion

The structural, mechanical, electronic and lattice dynamic properties of half-Heusler PdCoX (X = Si and Ge) alloys which conform to $F\bar{4}3m$ space group in each of α, β and γ phases have been investigated in detail. These alloys have been examined in three different atomic arrangements which are given by Wyckoff notation. We determined that both of our alloys are stable in β structural phase, however, γ phase can be considered as a secondary stable structural phase for these alloys. Both of our materials have metallic character due to the absence of band gaps in their spin-polarised electronic band structures. The calculated electronic band structures and total magnetic moments show that these alloys are close to ferromagnetic character in α phase and are close to non-magnetic behaviour in the other two phases. Also, some mechanical properties of these materials have been examined and it is clearly seen that these alloys are stable mechanically in β and γ phases, but unstable in α phase. Both of our alloys show anisotropic character mechanically in each stable phase. Finally, we examined the vibrational properties of these alloys in each structural phase. The phonon dispersion spectra of PdCoX (X = Si and Ge) alloys show that, both are stable dynamically in β and γ phases but unstable in α phase in agreement with the calculated elastic constants for each phase.

Disclosure statement

No potential conflict of interest was reported by the authors.

Funding

This work was supported by the Ahi Evran University Research Project Unit [project number PYO-KMY.4001.15.001].

References

[1] D. Xiao, Y. Yao, W. Feng, J. Wen, W. Zhu, X.Q. Chen, G.M. Stocks, and Z. Zhang, *Half-Heusler Compounds as a New Class of Three-Dimensional Topological Insulators*, Phys. Rev. Lett. 105 (2010), p. 096404.

[2] H. Lin, L.A. Wray, Y. Xia, S. Xu, S. Jia, R.J. Cava, A. Bansil, and M.Z. Hasan, *Half-Heusler ternary compounds as new multifunctional experimental platforms for topological quantum phenomena*, Nat. Mater. 9 (2010), pp. 546–549.

[3] I. Galanakis, K. Özdoğan, and E. Şaşıoğlu, *Ab initio electronic and magnetic properties of half-metallic NiCrSi and NiMnSi Heusler alloys: The role of defects and interfaces*, J. Appl. Phys. 104 (2008), p. 083916.

[4] H. Luo, Z. Zhu, G. Liu, S. Xu, G. Wu, H. Liu, J. Qu, and Y. Li, *Ab-initio investigation of electronic properties and magnetism of half-Heusler alloys XCrAl (X=Fe Co, Ni) and NiCrZ (Z=Al, Ga, In)*, Physica B: Condensed Matter 403 (2008), pp. 200–206.

[5] S. Kacimi, H. Mehnane, and A. Zaoui, *I-II–V and I–III–IV half-Heusler compounds for optoelectronic applications: Comparative ab initio study*, J. Alloys Compd. 587 (2014), pp. 451–458.

[6] S. Sakurada and N. Shutoh, *Effect of Ti substitution on the thermoelectric properties of (Zr, Hf)NiSn half-Heusler compounds*, Appl. Phys. Lett. 86 (2005), p. 082105.

[7] G. Rogl, P. Sauerschnig, Z. Rykavets, V.V. Romaka, P. Heinrich, B. Hinterleitner, A. Grytsiv, E. Bauer, and P. Rogl, *(V, Nb)-doped half Heusler alloys based on {Ti, Zr, Hf}NiSn with high ZT*, Acta Mater. 131 (2017), pp. 336–348.

[8] T. Graf, C. Felser, and S.S.P. Parkin, *Simple rules for the understanding of Heusler compounds*, Prog. Solid State Chem. 39 (2011), pp. 1–50.

[9] V. Jiban, K. Enamullah, and A. Alam, *Bismuth based Half Heusler Alloys with giant thermoelectric figure of merit*, J. Mater. Chem. A Mater. Energy Sustain. 5 (2016), pp. 1–9.

[10] R.A. de Groot, F.M. Mueller, P.G. Engen, and K.H.J. Buschow, *New class of materials: Half-metallic ferromagnets*, Phys. Rev. Lett. 50 (1983), pp. 2024–2027.

[11] D. Kieven, R. Klenk, S. Naghavi, C. Felser, and T. Gruhn, *I-II-V half-Heusler compounds for optoelectronics: Ab initio calculations*, Phys. Rev.B 81 (2010), p. 75208.

[12] T. Jungwirth, V. Novák, X. Martí, M. Cukr, F. Máca, A.B. Shick, J. Mašek, P. Horodyská, P. Němec, V. Holý, J. Zemek, P. Kužel, I. Němec, B.L. Gallagher, R.P. Campion, C.T. Foxon, and J. Wunderlich, *Demonstration of molecular beam epitaxy and a semiconducting band structure for I-Mn-V compounds*, Phys. Rev.B 83 (2011), p. 35321.

[13] P. Larson, S.D. Mahanti, and M.G. Kanatzidis, *Structural stability of Ni-containing half-Heusler compounds*, Phys. Rev.B 62 (2000), pp. 12754–12762.

[14] F.B. Mancoff, J.F. Bobo, O.E. Richter, K. Bessho, P.R. Johnson, R. Sinclair, W.D. Nix, R.L. White, and B.M. Clemens, *Growth and Characterization of Epitaxial NiMnSb/PtMnSb $C1_b$ Heusler alloy superlattices*, J. Mater. Res. 14 (1999), pp. 1560–1569.

[15] K. Mastronardi, D. Young, C.C. Wang, P. Khalifah, R.J. Cava, and A.P. Ramirez, *Antimonides with the half-Heusler structure: New thermoelectric materials*, Appl. Phys. Lett. 74 (1999), p. 1415.

[16] I. Galanakis, P. Mavropoulos, and P.H. Dederichs, *Electronic structure and Slater–Pauling behaviour in half-metallic Heusler alloys calculated from first principles*, J. Phys. D. Appl. Phys. 39 (2006), pp. 765–775.

[17] J. Toboła and J. Pierre, *Electronic phase diagram of the XTZ (X=Fe Co, Ni; T=Ti, V, Zr, Nb, Mn; Z=Sn, Sb) semi-Heusler compounds*, J. Alloys Compd. 296 (2000), pp. 243–252.

[18] L. Damewood, B. Busemeyer, M. Shaughnessy, C.Y. Fong, L.H. Yang, and C. Felser, *Stabilizing and increasing the magnetic moment of half-metals: The role of Li in half-Heusler LiMn Z (Z = N , P , Si)*, Phys. Rev. B 91 (2015), p. 064409.

[19] R.W.G. Wyckoff, *Crystal Structures*, Vol. 1, Wiley, New York, 1963.
[20] W. Huang, X. Wang, X. Chen, W. Lu, L. Damewood, and C.Y. Fong, *Structural and electronic properties of half-Heusler alloys PtXBi (with X=Mn, Fe, Co and Ni) calculated from first principles*, J. Magn. Magn. Mater. 377 (2015), pp. 252–258.
[21] L. Guan-Nan and J. Ying-Jiu, *First-principles study on the half-metallicity of half-Heusler alloys: XYZ (X = Mn, Ni; Y = Cr, Mn; Z = As, Sb)*, Chinese Phys. Lett. 26 (2009), p. 107101.
[22] S. Maheswari, S. Karthikeyan, P. Murugan, P. Sridhar, and S. Pitchumani, *Carbon-supported Pd-Co as cathode catalyst for APEMFCs and validation by DFT*, Phys. Chem. Chem. Phys. 14 (2012), pp. 9683–9695.
[23] R.M. Bozorth, P.A. Wolff, D.D. Davis, V.B. Compton, and J.H. Wernick, *Ferromagnetism in dilute solutions of cobalt in palladium*, Phys. Rev. 122 (1961), p. 1157.
[24] I. Galanakis, *High spin-polarization in ultrathin Co2MnSi/CoPd multilayers*, J. Magn. Magn. Mater. 377 (2015), pp. 291–294.
[25] G. Kresse and J. Hafner, *Ab initio molecular dynamics for liquid metals*, Phys. Rev.B 47 (1993), pp. 558–561.
[26] G. Kresse and J. Furthmüller, *Efficiency of ab initio total energy calculations for metals and semiconductors using a plane-wave basis set*, Comput. Mater. Sci. 6 (1996), pp. 15–50.
[27] P.E. Blöchl, *Projector augmented-wave method*, Phys. Rev.B 50 (1994), pp. 17953–17979.
[28] G. Kresse and D. Joubert, *From ultrasoft pseudopotentials to the projector augmented-wave method*, Phys. Rev.B 59 (1999), pp. 1758–1775.
[29] W. Kohn and L.J. Sham, *Self-Consistent Equations Including Exchange and Correlation*, Effects Phys. Rev. 140 (1965), p. A1133.
[30] P. Hohenberg and W. Kohn, *Inhomogeneous Electron Gas*, Phys. Rev. 136 (1964), p. B864.
[31] H.J. Monkhorst and J.D. Pack, *Special points for Brillouin-zone integrations*, Phys. Rev.B 13 (1976), pp. 5188–5192.
[32] P. Vinet, J.H. Rose, J. Ferrante, and J.R. Smith, *Universal features of the equation of state of solids*, J. Phys. Condens. Matter 1 (1989), pp. 1941–1963.
[33] J. Feng, B. Xiao, J.C. Chen, and C.T. Zhou, *Theoretical study on the stability and electronic property of Ag_2SnO_3*, Solid State Sci. 11 (2009), pp. 259–264.
[34] S.F. Matar, R. Weihrich, D. Kurowski, and A. Pfitzner, *DFT calculations on the electronic structure of $CuTe_2$ and Cu_7Te_4*, Solid State Sci. 6 (2004), pp. 15–20.
[35] E. Zhao and Z. Wu, *Electronic and mechanical properties of 5d transition metal mononitrides via first principles*, J. Solid State Chem. 181 (2008), pp. 2814–2827.
[36] Y. Le Page and P. Saxe, *Symmetry-general least-squares extraction of elastic coefficients from ab initio total energy calculations*, Phys. Rev.B 63 (2001), p. 174103.
[37] F. Mouhat and F.X. Coudert, *Necessary and sufficient elastic stability conditions in various crystal systems*, Phys. Rev.B 90 (2014), p. 224104.
[38] D.H. Wu, H.C. Wang, L.T. Wei, R.K. Pan, and B.Y. Tang, *First-principles study of structural stability and elastic properties of MgPd3 and its hydride*, J. Magnes. Alloys 2 (2014), pp. 165–174.
[39] D. Pettifor, *Theoretical predictions of structure and related properties of intermetallics*, Mater. Sci. Technol. 8 (1992), pp. 345–349.
[40] A.V. Ponomareva, E.I. Isaev, Y.K. Vekilov, and I.A. Abrikosov, *Site preference and effect of alloying on elastic properties of ternary B 2 NiAl-based alloys*, Phys. Rev.B 85 (2012), p. 144117.
[41] W. Voigt, *Lehrbuch der Kristallphysik [The textbook of crystal physics]*, B.G. Teubner, Leipzig und Berlin, 1928.
[42] A. Reuss, *Berechnung der Fliessgrenze von Mischkristallen auf Grund der Plastizitatsbedingung fur Einkristalle [Calculation of the liquid limit of mixed crystals on the basis of the plasticity condition for single crystals]*, J. Appl. Math. Mech. 9 (1929), pp. 49–58.

[43] R. Hill, *The elastic behaviour of a crystalline aggregate*, Proc. Phys. Soc. Sect. A 65 (1952), pp. 349–354.
[44] H. Ozisik, E. Deligoz, K. Colakoglu, and G. Surucu, *Mechanical and lattice dynamical properties of the Re_2C compound*, Phys. Status Solidi – Rapid Res. Lett. 4 (2010), pp. 347–349.
[45] D. Li, T. Jaglinski, D.S. Stone, and R.S. Lakes, *Temperature insensitive negative Poisson's ratios in isotropic alloys near a morphotropic phase boundary*, Appl. Phys. Lett. 101 (2012), p. 251903.
[46] G.N. Greaves, A.L. Greer, R.S. Lakes, and T. Rouxel, *Poisson's ratio and modern materials*, Nat. Mater. 10 (2011), pp. 823–837.
[47] G. Surucu, C. Kaderoglu, E. Deligoz, and H. Ozisik, *Investigation of structural, electronic and anisotropic elastic properties of Ru-doped WB2 compound by increased valence electron concentration*, Mater. Chem. Phys. 189 (2017), pp. 90–95.
[48] K. Lau and A.K. McCurdy, *Elastic anisotropy factors for orthorhombic, tetragonal, and hexagonal crystals*, Phys. Rev.B 58 (1998), pp. 8980–8984.
[49] E. Schreiber, O.L. Anderson, and N. Soga, *Elastic Constants and their Measurements*, McGraw-Hill, New York, 1973.
[50] O.L. Anderson, *A simplified method for calculating the debye temperature from elastic constants*, J. Phys. Chem. Solids 24 (1963), pp. 909–917.
[51] E. Deligöz, K. Çolakoğlu, Y.Ö. Çiftçi, and H. Özişik, *Electronic, elastic, thermodynamical, and dynamical properties of the rock-salt compounds LaAs and LaP*, J. Phys. Condens. Matter 19 (2007), p. 436204.
[52] A. Togo and I. Tanaka, *First principles phonon calculations in materials science*, Scr. Mater. 108 (2015), pp. 1–5.
[53] S. Baroni, P. Giannozzi, and A. Testa, *Green's-function approach to linear response in solids*, Phys. Rev. Lett. 58 (1987), pp. 1861–1864.
[54] X. Gonze and J.P. Vigneron, *Density-functional approach to nonlinear-response coefficients of solids*, Phys. Rev.B 39 (1989), pp. 13120–13128.
[55] X. Gonze, D.C. Allan, and M.P. Teter, *Dielectric tensor, effective charges, and phonons in α-quartz by variational density-functional perturbation theory*, Phys. Rev. Lett. 68 (1992), pp. 3603–3606.